Chemical Science

Accepted Manuscript

This article can be cited before page numbers have been issued, to do this please use: R. Wang, W. Yang, M. Su, J. Qin, J. Liu, X. Yan, J. Cao, R. Yuan, Y. Zhuo, M. Chen, C. Yang and W. Liang, *Chem. Sci.*, 2025, DOI: 10.1039/D5SC04624F.

ROYAL SOCIETY OF CHEMISTRY

rsc.li/chemical-science

View Article Online
DOI: 10.1039/D5SC04624F

ARTICLE

Structural Reorganization-based Catalytic Hairpin Assembly Enable Small Molecule Monitoring in Living Cell

Received 00th January 20xx,
Accepted 00th January 20xx

DOI: 10.1039/x0xx00000x

Rui-Wen Wang, [†a] Wei-Guo Yang, [†a] Ming-Li Su,[a] Jia-Min Qin,[a] Jia-Qi Liu,[c] Xiao-Han Yang [a], Jun-Yi Cao, [a] Ruo Yuan[a], Ying Zhuo,*[a] Ming Chen,*[c] Chaoyong Yang,*[b] and Wen-Bin Liang*[a]

Small-molecule drugs, constituting over 60% of FDA-approved therapeutics (2017–2022), face unresolved challenges in elucidating intracellular mechanism. We present a dual-strategy platform integrating "In Silico Aptamer Affinity Maturation" (ISAAM) and "Structural Reorganization-Catalytic Hairpin Assembly" (SR-CHA). ISAAM computationally designs high-affinity aptamers, while SR-CHA eliminates undesired signals via energy-minimized conformational control, achieving a signal-to-background improvement over conventional CHA. This system enables ultrasensitive small molecule monitoring in live cells, resolving traditional challenges of false positives and inefficiency. Demonstrated through intracellular imaging and kinetic studies, SR-CHA offers a robust tool for probing small molecule interactions in biological systems, advancing drug discovery and diagnostic applications.

Introduction

Small molecules are ubiquitous in nature as the basic unit to play important constituent and regulatory roles in living systems.[1-3] Meanwhile, numerous synthetic small molecules as drug to regulate life processes *via* adaptable routes. More than 60% of new chemical entities approved by the US Food and Drug Administration (FDA) are small molecular drugs (2017-2022).[4] Small molecules are expected to drive innovation in future drug discovery, performing great significance in exploring the biological mechanisms of small molecules in vivo.[5-8] Whereas, the biological mechanisms for most of the small molecules are still in doubt, which primarily stems from three key factors: firstly, conventional detection methodologies for small molecules frequently necessitate harsh reaction conditions; secondly, achieving specific molecular recognition and efficient signal transduction presents significant technical challenges; thirdly, the majority of small molecules cannot function as enzymatic substrates or participate in enzyme-associated reaction pathways. With chloramphenicol (CAP) as a model, which is a highly effective broad-spectrum antibiotic with strong inhibitory effects against both Gram-positive and negative bacteria that has been confirmed by in vitro bacteriostatic tests and extensive clinical trials and applications.[9] Nevertheless, CAP with enormous toxic effects could be readily enriched in animals and humans, and may cause irreversible myelosuppressive reactions leading to aplastic anaemia.[10-12] While high-performance liquid chromatography (HPLC), liquid chromatography-tandem mass spectrometry (LC-MS), and paper-based antibiotic sensors (PAS) have demonstrated significant analytical advantages for CAP detection,[13-16] substantial technical challenges persist in developing reliable methods for monitoring CAP in living cellular systems. Consequently, accurately and sensitively monitoring the intracellular concentration and distribution of CAP remains a significant challenge, which hinders the elucidation of its underlying biological mechanisms.[17] This limitation underscores the urgent need for detection methodologies that combine target specificity with intracellular environmental adaptability.

To address this demand, aptamer-based strategies show unique advantages and potentials in the field of bioanalytical chemistry of small molecules. Their inherent target recognition specificity and structural programmability could convert small molecules recognition into nucleic acid structural information, generating a great deal of application value in specific and sensitive analysis of small molecules.[16, 18-20] However, the current aptamer selection methodology exhibits notable limitations in its flexibility. A significant challenge lies in the stringent screening process to identify specific aptamers from combinatorial libraries containing approximately 10^{14} to 10^{15} distinct molecular species.[21, 22] To illustrate this limitation quantitatively with the selection of a 40-nucleotide aptamer as a representative case, there are 4^{40} different sequences and obviously, the probability to select the optimal one is approximately 1 in 10^9, that is remarkably low, being several orders of magnitude below the chance of winning a typical lottery jackpot.

[a.] *Key Laboratory of Luminescence Analysis and Molecular Sensing (Southwest University), Ministry of Education, Institute of Developmental Biology and Regenerative Medicine, College of Chemistry and Chemical Engineering, Southwest University, Chongqing 400715, P. R. China. E-mail: wenbinliangasu@gmail.com.*
[b.] *Institute of Molecular Medicine, Shanghai Key Laboratory for Nucleic Acid Chemistry and Nanomedicine, State Key Laboratory of Oncogenes and Related Genes, School of Medicine, Shanghai Jiao Tong University, Shanghai, 200127, China. Email: cyyang@xmu.edu.cn.*
[c.] *Department of Clinical Laboratory Medicine, Southwest Hospital, Third Military Medical University (Army Medical University), Chongqing 400038, China. Email: chming1971@126.com*

View Article Online
DOI: 10.1039/D5SC04624E

While increasing library capacity represents a theoretically feasible approach to enhance the probability of identifying optimal aptamers, the associated temporal and resource requirements render this strategy practically unsustainable. On the other hands, in the case of small-molecule-targeting aptamers, the design parameters for nucleic acid conformational modifications are significantly constrained by the limited availability of binding sites. This restriction presents a substantial challenge in achieving an optimal equilibrium between binding affinity and structural stability.[23-26] Furthermore, the compromised stability of nucleic acid structures may result in elevated background signal interference, thereby potentially compromising the reliability of detection systems. To fully exploit small molecule binding sites, we propose the In Silico Aptamer Affinity Maturation (ISAAM) method, which analyses the binding modes of small molecule parent compounds with aptamers and provides guidance for aptamer design. Recently, we have investigated the structure and interaction analysis of HBC aptamers for artificial aptamers.[27] This provides the basis for the design of artificial aptamer affinity maturation, which is expected to yield high-affinity aptamers through design and reconstruction based on existing small-molecule aptamers obtained through screening.

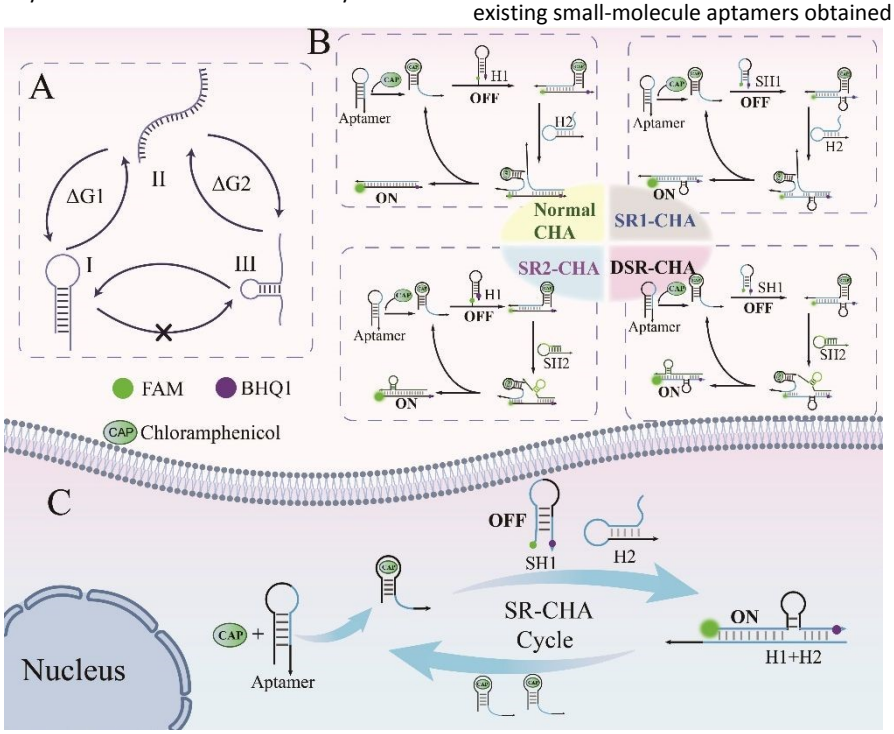

Fig.1 Schematic diagram of the small molecule-initiated SR-CHA for amplified detection of CAP. (A) Schematic diagram of the transformation of nucleic acid chains with different structures. (B) Schematic diagram of the cyclic process of small molecule-initiated Normal-CHA and SR-CHAs. (C) Intracellular SR1-CHA cycle process.

On the other hand, efficient signal amplification strategies are indispensable in high-sensitivity analyses, particularly for small molecules exhibiting low binding energies to their aptamers. Catalytic hairpin assembly (CHA),[28-32] an enzyme-free nucleic acid amplification technique, employs toehold-mediated strand displacement (TMSD) under mild reaction conditions,[22, 33, 34] to achieve a theoretically predicted 10^6 fold acceleration in chain displacement kinetics, thereby establishing itself as a preeminent methodology in aptamer-mediated signal recognition-conversion systems. However, the obvious inherent flaws could not be ignored in the CHA strategy. Even in the absence of a elicitation chain, the hairpins in the CHA circuit may react non-specifically that reduces the Signal-to-Background Ratio (SBR) significantly.[35-37] Although several strategies, including mismatch-based approaches [35, 38, 39] have been developed to mitigate CHA signalling leakage, the incorporation of such modifications often compromises reaction efficiency and specificity. Significant challenges remain in developing CHA systems that simultaneously achieve low background noise and high efficiency for reliable in vivo small-molecule detection.[40]

To address these challenges, we developed a small-molecule-triggered Structural Reorganization-CHA (SR-CHA) system, enabling precise monitoring of CAP in both living cells and in vitro environments. This integrated approach combines two key innovations. Firstly, an ISAAM-based aptamer augmentation technology enables high-affinity small molecule recognition through molecular-nucleic acid sequence conversion. On the other hand, a nucleic acid SR-CHA amplification strategy addresses signal-to-background ratio (SBR) limitations by minimizing unintended binding. The SR-CHA method demonstrates significant advantages in intracellular small molecule analysis, offering reduced background interference compared to conventional CHA systems while maintaining high efficiency under physiological conditions. This advancement provides a robust platform for investigating CAP's intracellular mechanisms and distribution patterns.

Results and Discussion

Aptamer optimization based on ISAAM method.

On the basis of Aptamer 0 (Fig.2A), a known aptamer of CAP,[41, 42] the number of bases bound to its stem was adjusted to increase the stability of the aptamer. The thermodynamic schematic diagram of the states in which different structures of the aptamer is shown in Fig.2F. The thermodynamic stability of the aptamer system is primarily governed by ΔG2, which originates from the stem base-pairing energy. To minimize background signals resulting from spontaneous transitions to the linear state, the absolute value of ΔG2 must be sufficiently large relative to ΔG1. Simultaneously, structural modifications must preserve the integrity of the CAP binding site. Guided by these thermodynamic principles and structural considerations, we engineered three optimized aptamer variants through targeted base substitutions at non-CAP binding regions: (1) Aptamer1 (Fig.2B) with G11C substitution, (2) Aptamer2 (Fig.2C) with T13A substitution, and (3) Aptamer3 (Fig.2D) containing both G11C and T13A substitutions.

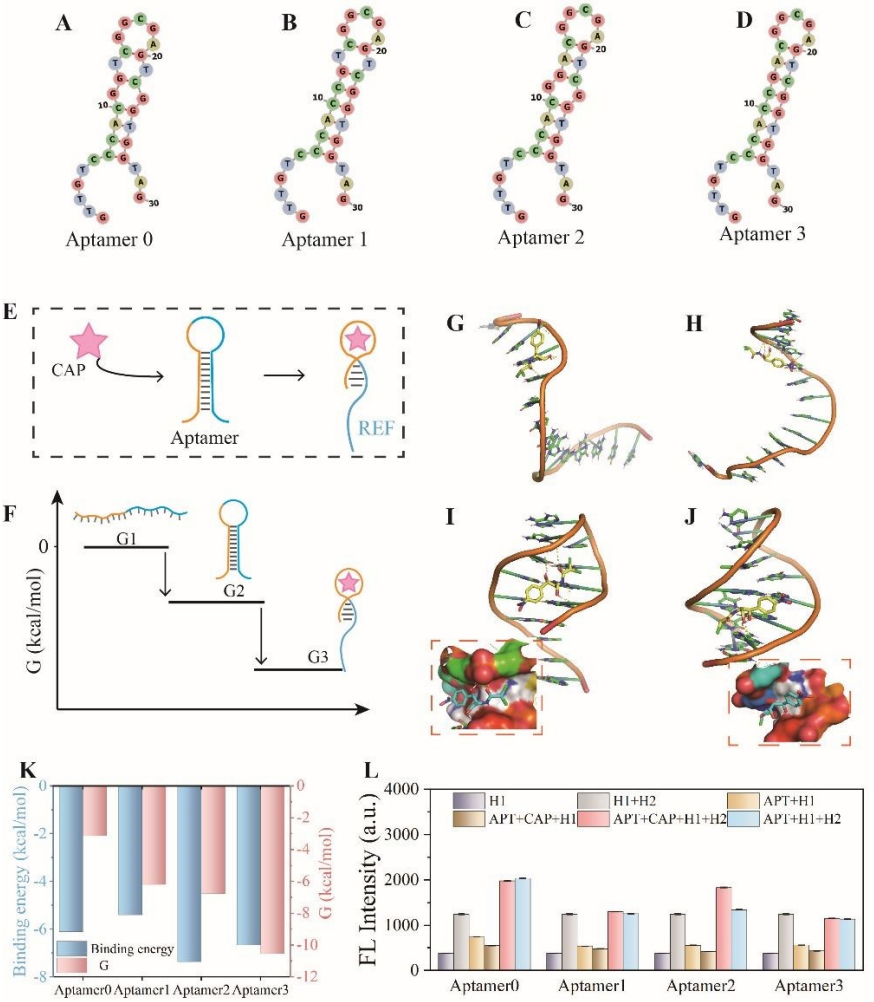

Fig.2 Initial aptamer of CAP, Aptamer 0 (A) and replace its 11G base with C, obtained Aptamer 1 (B), replace its 13T base with A, obtained Aptamer 2 (C), and change both 11G and 13T to get Aptamer 3 (D). (E) Schematic of the conformational change that occurs when the aptamer binds to the CAP. (F) Energy changes during conformational transitions of the aptamer. (G-J) Results of docking with CAP after removal of the ref part of the aptamers and its docking domain with CAP. (K) Binding energy of Aptamer 0, 1, 2, 3 to CAP docking and free energy (G) of each aptamer. (L) Fluorescence experiments with the four aptamers with 500 nM CAP.

These modifications achieved dual objectives: reducing structural instability-induced signal leakage and increasing binding site accessibility. Quantitative analysis of the thermodynamic stability revealed enhanced free energy values for all optimized aptamers, as demonstrated in Fig.2K. When CAP binds to the aptamer, interaction of small molecules results in the structural shift of the aptamer, exposing the 16G to 27G region (REF) and triggering the subsequent CHA reaction. To investigate the ability of the four aptamers to release the REF portion upon binding to CAP, the REF portion of the aptamer was deleted and the remaining portion (CAP reaction domain) was used to dock to CAP, and the results of the docking are showed in Fig.2G-J. It can be seen in Fig.2I and J that the remaining portion of aptamer 2 and 3 binds to CAP with a large change in chain morphology, forming a binding domain capable of encapsulating CAP. Furthermore, we analysed CAP-aptamer binding energies *via* Autodock 4 and aptamer-specific Gibbs free energies from NUPACK webserver. The binding energy of aptamer 2 to CAP reached -7.37 kcal/mol, which is significantly better than the other three aptamers (Fig.2K). Considering the stability of the aptamer and the magnitude of binding energy to the small molecules of the target, aptamer 2 has superior performance at present.

On the optimized conditions (Figure S3), the superior performance of Aptamer 2 was further confirmed by fluorescence experiments (Fig.2L). As can be seen in the figure, Aptamer 2 was able to achieve a significantly enhanced signal above the background value. Aptamer 2 was selected for all subsequent experiments based on its superior binding affinity and stability compared to other candidates.

Thermodynamic models and thermodynamic analysis of SR-CHA and conventional CHA.

To elucidate the mechanistic details and intermediate states associated with branch migration in SR-CHA systems, we conducted a comparative thermodynamic analysis between SR-CHA and conventional CHA. Toehold-Mediated Strand Displacement (TMSD) is a fundamental nucleic acid reaction process in which a single-stranded (ss) nucleic acid invader strand initiates binding at a terminal overhang region (toehold) of a double-stranded DNA (dsDNA) complex, subsequently displacing the incumbent strand through a branch migration mechanism (Fig.3A). [43] Niranjan Srinivas [44] built a thermodynamic model for a TMSD process (Fig.3B). They model branch migration at a detailed level that explicitly includes intermediates, thereby highlighting important thermodynamic features of the process that are not evident from the phenomenological approach.

On the basis of this thermodynamic model, we can analyse the thermodynamic processes of structural CHA and normal CHA. For all four CHAs mentioned above, the first step is to bind to CAP and then deform the aptamer to expose the part that triggers the next step of CHA. Here, to simplify the representation, we omit the deformation step and directly represent the trigger chain with the blue part shown in the figures. For the conventional CHA process, the trigger first binds to the toehold of H1, after which it opens the stem of the H1 hairpin to form the H1-trigger complex, and next, H2 binds to the toehold of H1, displacing the Trigger and allowing the cycle to continue. The thermodynamic changes of this process are shown in Fig.3C and all specific values of free energy (G) in the figures are from NUPACK. However, in the thermodynamic process of SR1-CHA, as depicted in Fig.3D, the binding of the trigger induces the structural reorganization of SH1 to form a Structural-reorganization Work Unit (SWU). The interaction between the reconfigured SH1 and the trigger exhibits a lower ΔG, which significantly mitigates signal leakage associated with the CHA process. Afterwards, H2 binds to the SH1-trigger complex and releases the trigger, allowing the trigger to continue the cycle.

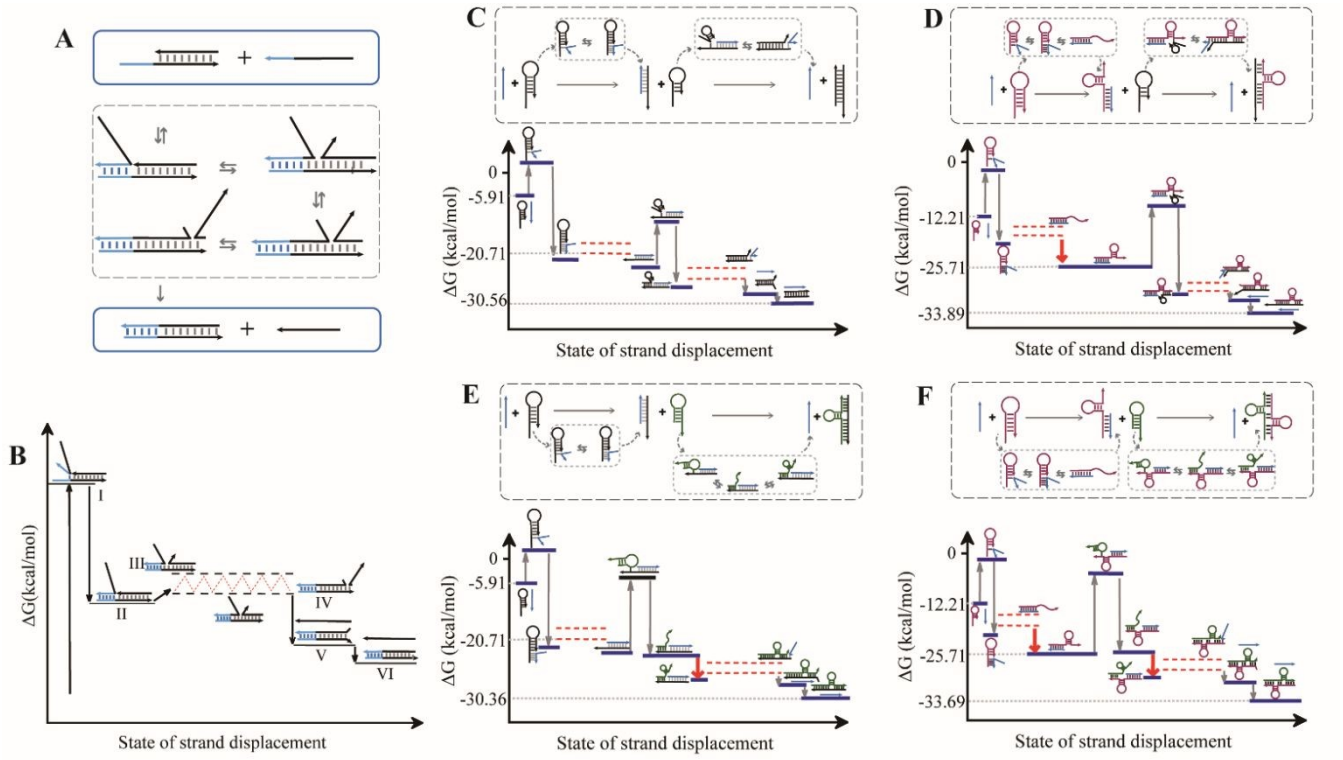

Fig. 3 (A) Schematic illustration of a toehold-mediated strand displacement process. (B) Free energy modelling of a toehold mediated strand displacement process. (C-F) Processes of free energy changes in different steps of normal CHA (C), SR1-CHA (D), SR2-CHA (E) and DSR-CHA (F).

This reduction in ΔG enhances the thermodynamic stability of the system, thereby improving the overall fidelity and efficiency of the reaction. In the SR2-CHA system (Fig.3E), while the H1 hairpin maintained its structural integrity, the SH2 component exhibited a conformational rearrangement upon recognizing the toehold binding region of the H1-trigger complex, resulting in the formation of a stable SWU structure. This structural reorganization induced a substantial decrease in the ΔG of the system, thereby enhancing its thermodynamic stability. Subsequently, SH2 fully binds to H1, releasing the trigger to re-enter the CHA cycle, thereby enabling

continuous signal amplification and improving the efficiency of the reaction. Through the strategic integration of SR1-CHA and SR2-CHA mechanisms, we developed a dual-structural reorganization CHA (DSR-CHA) system that incorporates two metastable structural transformation processes. This design integrates two sequential metastable structural transitions that cooperatively suppress undesired background signals through energy landscape optimization, theoretically enabling better background reduction efficiency compared to conventional CHA systems, as shown in Fig.3F.

Kinetic analysis of small molecules induced SR CHA and normal CHA.

The real-time fluorescence experiments were furtherly employed to investigate the kinetic characteristics of SR-CHA. As shown in Fig. 4A, non-fluorescence-labelled strands were first introduced into cuvettes and then excited at 497 nm for 600 s. Since no fluorescent strands were present, this period established both a near-zero baseline and a zero-background signal for the first 600 seconds. At precisely 600 s, fluorescence-labeled strands were simultaneously introduced to all reaction systems. This protocol ensured quantitatively comparable initial signal levels between CAP-positive and CAP-negative groups during real-time fluorescence monitoring, thus preventing signal discrepancies arising from baseline inconsistencies. Upon the introduction of H1, which was labelled with FAM and BHQ1, a gradual increase in fluorescent signals was observed following the establishment of a stable baseline. The fluorescence intensity at an emission wavelength of 520 nm was monitored in real time over a period of 6,000 s. Figs.4B-E show the kinetic performance of normal CHA, SR1-CHA, SR2-CHA and DSR-CHA, respectively. In the conventional CHA system, the introduction of CAP induces a significant enhancement in fluorescence intensity compared to the CAP-free control, with the signal reaching saturation at approximately 4,000 s. Beyond this time point, the fluorescence intensity stabilizes, exhibiting no further temporal increase, and a constant $(F\text{-}F_0)/F_0$ ratio is maintained. For SR1-CHA, although its fluorescence signal intensity is not as strong as that of normal CHA and shows a slower increase in kinetics, it can be seen in Figs.4C that the fluorescence signal of the CAP-positive group is still on an increasing trend as of 6,000 s, whereas the background signal shows a stabilizing trend earlier. In this regard, it can be hypothesized that the kinetic response of the reaction is slowed down due to the metathesis process of SH1, but SR1-CHA performs a superior kinetic potential. Compared to conventional CHA, SR1-CHA also exhibited higher $(F\text{-}F_0)/F_0$ values, further demonstrating its capacity to reduce the CHA response background. For SR2-CHA, it demonstrated a much faster response compared to normal CHA, reaching a stable high signal value in about 2,500 s, while the $(F\text{-}F_0)/F_0$ value of the response was significantly better than that of normal CHA. For DSR-CHA, as predicted previously for the reaction, DSR-CHA exhibits an extremely slow growth trend in kinetics, and even with a reaction time of 6,000 s, it is still difficult to visualize the growth of the fluorescence signal, and although it also achieves higher $(F\text{-}F_0)/F_0$ values, the overall signal is pretty low.

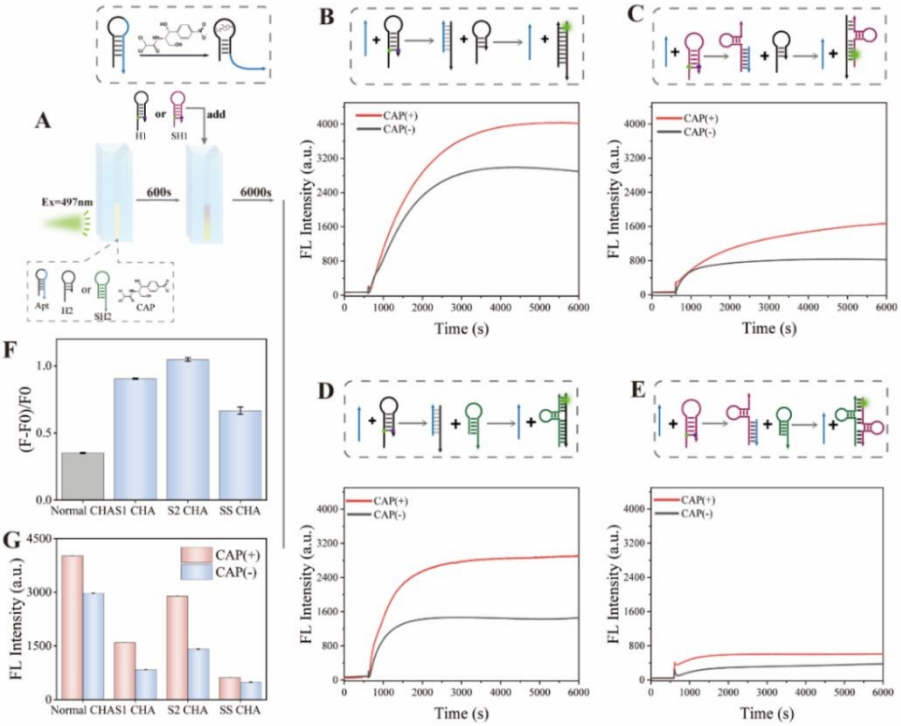

Fig.4 (A) Schematic diagram of the kinetic experiment process. Dynamic fluorescence signal of (B) normal CHA, (C) SR1-CHA, (D) SR2-CHA and (E) DSR-CHA within 6,000 s at 37 °C. (F) Comparison of $(F\text{-}F_0)/F_0$ values for the four CHA systems. (G) CAP negative and positive fluorescence signal values for the four CHAs after hybridization at 37 °C for 2 h.

From a kinetic analysis of the four CHA systems, distinct reaction characteristics were observed. In SR1-CHA, the structural reorganization primarily occurs at SH1, resulting in a relatively slower reaction kinetics. Although the fluorescence intensity achieved

within 6,000 s is limited, this system demonstrates considerable reaction potential, suggesting that extended reaction duration could yield improved $(F\text{-}F_0)/F_0$ values. In contrast, SR2-CHA exhibits superior kinetic performance due to its partial structural reorganization at SH2, which not only maintains reaction velocity, but also demonstrates enhanced background suppression. Although theoretical predictions suggested that the DSR-CHA system could exhibit optimal reaction performance, its kinetic efficiency is substantially limited by the concurrent structural reorganization processes required at both SH1 and SH2 domains. This dual-site conformational rearrangement introduces thermodynamic barriers that impede the progression of the catalytic reaction.

Performance Comparison of Conventional CHA and SR-CHA in CAP Analysis.

On optimal conditions, the performance of the proposed SR-CHA for the detection of CAP was examined (Figs.S9 A-D). Different concentrations of CAP were detected with the four CHA detection systems. It was observed that the fluorescence intensity exhibited a gradual increase as the concentration of CAP ranged from 1 pM to 100 nM (Fig.S9 E-H). As demonstrated in Fig.S9 I-L, for all four CHA systems, there was an increase in the $(F\text{-}F_0)/F_0$ ratio with a rise in the concentration of CAP, and the ratio was linearly associated with lg c_{CAP} in the range of 1 pM to 100 nM, and showed linearity in the detection of CAP. The Pearson's correlation coefficients r for SR1-CHA and SR2-CHA were calculated as 0.9918 and 0.9932, respectively, exceeding that of conventional CHA (r = 0.9565), which demonstrates that the SR-CHA system exhibits superior linearity in CAP detection compared to the conventional counterpart. Furthermore, SR1-CHA and SR2- CHA can achieve higher$(F\text{-}F_0)/F_0$ ratios and with a 2.5~3 times higher sensitivity, which implies that our proposed SR-CHA has a superior ability to improve detection performance. Additionally, practical validation using real samples (honey and milk) also yielded robust detection results, as illustrated in Fig.S10. These results suggest that SR-CHA strategy has a great potential for application in CAP analysis of real samples. It is noteworthy that the $(F\text{-}F_0)/F_0$ ratio exhibited by DSR-CHA is found to approximate that of the regular CHA, a result that is rather unexpected. However, this phenomenon suggests that for DSR-CHA, although the background can be effectively reduced to a certain extent, the kinetic effects in the reaction should not be neglected, and the formation of two SWUs by SH1 and SH2 in DSR-CHA leads to the detection of small molecules with a reduction in sensitivity, in which a longer reaction time may be necessary for sensitive analysis.

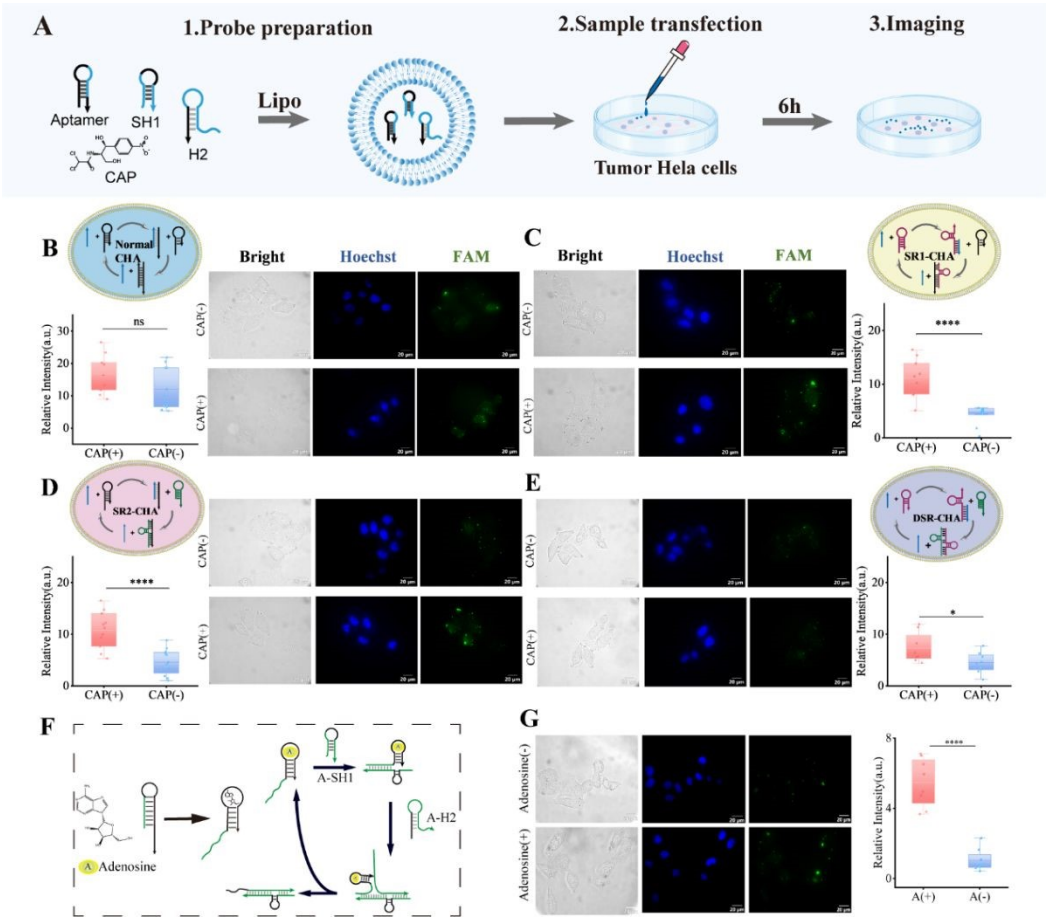

Fig.5 (A) Schematic diagram of intracellular imaging steps. Fluorescence imaging of normal CHA (B) SR1-CHA (C) SR2-CHA (D) and DSR-CHA (E) in Hela cells. (F) Schematic diagram of the adenosine-mediated SR1-CHA process. (B) Selectivity of SR1-CHA toward adenosine. (G) Fluorescence imaging of SR1-CHA to detect adenosine intracellularly.

Small Molecule Imaging in Living Cells based on Conventional CHA and SR-CHA.

To explore the intracellular expression of structural SR-CHA, we fluorescently imaged conventional CHA and three SR-CHA systems in

cervical cancer (HeLa) cells. The behaviour of the four CHA systems in HeLa cells was consistent with the fluorescence signals measured in vitro. In traditional CHA systems (Fig. 5B), while the CAP-containing experimental group generated somewhat higher FAM signals than the blank group, the blank controls themselves showed significant background interference. For the structural SR1-CHA (Fig.5C) and SR2-CHA (Fig.5D), setting up the experimental group with CAP and the blank group with TE buffer instead of CAP, both experimental groups produced FAM fluorescence signals significantly higher than the background. However, for DSR-CHA (Fig.5E), which is also a structural reorganization-based CHA, both experimental and control groups only triggered lower fluorescence signals, and there was no obvious difference in signal intensity between the experimental and control groups. The intracellular imaging experiments illustrate that the SR-CHA strategy is not only suitable for in vitro assays, but also has the potential to perform intracellular assays, which highlight the versatility and broad applicability of the SR-CHA strategy, paving the way for its future use in complex biological systems and clinical diagnostics.

Application of SR-CHA strategy to the detection of adenosine molecules.

In order to demonstrate the general applicability of SR-CHA strategy and expand its scope of application, we redesigned the SR1-CHA cycle using adenosine (A) molecules as targets and evaluated the performance of this reaction. The schematic diagram of the SR1-CHA system mediated with adenosine is shown in Fig.5F, in which the detection performance of the CHA system showed promising results, both in terms of selectivity and linearity (Fig.S11). In addition, we also performed intracellular fluorescence imaging experiments, found that adenosine-mediated SR1-CHA also possessed favourable ability to detect adenosine in cells. As shown in Fig.5G, the negative-positive fluorescence imaging results of intracellular adenosine were significantly diverged from the negative-positive fluorescence imaging results, which confirms the universality of our proposed SR-CHA strategy. Therefore, we anticipate that through rational sequence design tailored to specific small molecules, an efficient detection strategy with minimal background interference can be developed. This approach holds significant potential for both in vivo and in vitro applications, enabling highly sensitive and specific detection of small molecules.

Conclusions

In conclusion, we have established a novel SR-CHA strategy for sensitive small molecule detection. The enhanced performances of this approach were systematically validated through comprehensive fluorescence assays, kinetic studies, thermodynamic characterization, and intracellular imaging applications. Comparative analysis with conventional CHA systems revealed distinct advantages of the SR-CHA strategy. The SR-CHA strategy demonstrates three significant advantages over conventional CHA systems: (1) enhanced molecular specificity and detection sensitivity for small molecule targets, (2) substantially reduced background signal through the elimination of self-hybridization artifacts characteristic of traditional two-strand CHA systems, and (3) improved cellular imaging capability coupled with superior circuit efficiency in biological environments. We envision that this innovative strategy will provide a versatile platform for advanced biosensing applications, enabling both fundamental bioanalytical research in vivo and mechanistic investigations of small molecule interactions at the cellular level.

Author contributions

R.W., and W.Y. contributed equally to this work. W.L. designed research; R.W., W.Y., and J.Q., performed research; R.W., W.Y., M.S., J.L., X.Y., J.C., and R.Y., analysed data; W.L., Y.Z., M.C., and C.Y., supervised the work; R.W., W.Y. and W.L. wrote the paper. All authors read and approved the final manuscript.

Conflicts of interest

There are no conflicts to declare.

Data availability

All the data supporting the findings of this study are available within the article and can be obtained from the corresponding author upon reasonable request.

Acknowledgements

This work was financially supported by the Chongqing Municipal Science and Health Joint Medical Research Key Project (2025DBXM004) and National Natural Science Foundation (NNSF) of China (81972024). We would like to express our gratitude for the assistance provided by Yan Li and Lan Xu (Analytical & Testing Centre, Southwest University).

References

1. S. Qiu, Y. Cai, H. Yao, C. Lin, Y. Xie, S. Tang and A. Zhang, Small molecule metabolites: discovery of biomarkers and therapeutic targets, *Signal Transduction and Targeted Therapy*, 2023, **8**.
2. S. Qiu, Y. Cai, Z. Wang, Y. Xie and A. Zhang, Decoding functional significance of small molecule metabolites, *Biomedicine & Pharmacotherapy*, 2023, **158**.
3. A. Gutteridge, M. Kanehisa and S. Goto, Regulation of metabolic networks by small molecule metabolites, *BMC Bioinformatics*, 2007, **8**.
4. P. Bhutani, G. Joshi, N. Raja, N. Bachhav, P. K. Rajanna, H. Bhutani, A. T. Paul and R. Kumar, U.S. FDA Approved Drugs from 2015-June 2020: A Perspective, *Journal of medicinal chemistry*, 2021, **64**, 2339-2381.
5. L. M. Mustachio, A. Chelariu-Raicu, L. Szekvolgyi and J. Roszik, Targeting KRAS in Cancer: Promising Therapeutic Strategies, *Cancers*, 2021, **13**.
6. D. R. Owen, C. M. N. Allerton, A. S. Anderson, L. Aschenbrenner, M. Avery, S. Berritt, B. Boras, R. D. Cardin, A. Carlo, K. J. Coffman, A. Dantonio, L. Di, H. Eng, R. Ferre, K. S. Gajiwala, S. A. Gibson, S. E.

Greasley, B. L. Hurst, E. P. Kadar, A. S. Kalgutkar, J. C. Lee, J. Lee, W. Liu, S. W. Mason, S. Noell, J. J. Novak, R. S. Obach, K. Ogilvie, N. C. Patel, M. Pettersson, D. K. Rai, M. R. Reese, M. F. Sammons, J. G. Sathish, R. S. P. Singh, C. M. Steppan, A. E. Stewart, J. B. Tuttle, L. Updyke, P. R. Verhoest, L. Wei, Q. Yang and Y. Zhu, An oral SARS-CoV-2 M(pro) inhibitor clinical candidate for the treatment of COVID-19, *Science (New York, N.Y.)*, 2021, **374**, 1586-1593.

7. M. Y. Fang, S. Markmiller, A. Q. Vu, A. Javaherian, W. E. Dowdle, P. Jolivet, P. J. Bushway, N. A. Castello, A. Baral, M. Y. Chan, J. W. Linsley, D. Linsley, M. Mercola, S. Finkbeiner, E. Lecuyer, J. W. Lewcock and G. W. Yeo, Small-Molecule Modulation of TDP-43 Recruitment to Stress Granules Prevents Persistent TDP-43 Accumulation in ALS/FTD, *Neuron*, 2019, **103**, 802-819.e811.

8. J. Li, X. Yao, J. Ma, C. Liu, W. Hong, H. Wu, M. Li and L.-H. Guo, Recent advances in the electrochemiluminescence detection of small molecule drugs, *The Analyst*, 2025, DOI: 10.1039/d4an01562b.

9. Y. Sun, G. I. N. Waterhouse, X. Qiao, J. Xiao and Z. Xu, Determination of chloramphenicol in food using nanomaterial-based electrochemical and optical sensors-A review, *Food Chemistry*, 2023, **410**, 135434.

10. E. Nordkvist, T. Zuidema, R. G. Herbes and B. J. A. Berendsen, Occurrence of chloramphenicol in cereal straw in north-western Europe, *Food Additives & Contaminants: Part A*, 2016, **33**, 798-803.

11. H. Tsai, H. C. Hu, C. C. Hsieh, Y. H. Lu, C. H. Chen and C. B. Fuh, Fluorescence studies of the interaction between chloramphenicol and nitrogen‐doped graphene quantum dots and determination of chloramphenicol in chicken feed, *Journal of the Chinese Chemical Society*, 2019, **67**, 152-159.

12. S. Deng, F. Wang, Y. Li, J. Li, J. Zhan, Y. Shen, Z. Peng, C. Song, R. Cai, H. Yang and W. Tan, Triple Helix Molecular Switch Cascade Multiple Signal Amplification Strategies for Ultrasensitive Chloramphenicol Detection, *Analytical Chemistry*, 2024, **96**, 20312-20317.

13. X. Wang, J. Li, D. Jian, Y. Zhang, Y. Shan, S. Wang and F. Liu, Paper-based antibiotic sensor (PAS) relying on colorimetric indirect competitive enzyme-linked immunosorbent assay for quantitative tetracycline and chloramphenicol detection, *Sensors and Actuators B: Chemical*, 2021, **329**, 129173.

14. H. Kikuchi, T. Sakai, R. Teshima, S. Nemoto and H. Akiyama, Total determination of chloramphenicol residues in foods by liquid chromatography-tandem mass spectrometry, *Food Chemistry*, 2017, **230**, 589-593.

15. H. N. Jung, D. H. Park, Y. J. Choi, S. H. Kang, H. J. Cho, J. M. Choi, J. H. Shim, A. A. Zaky, A. M. Abd El-Aty and H. C. Shin, Simultaneous Quantification of Chloramphenicol, Thiamphenicol, Florfenicol, and Florfenicol Amine in Animal and Aquaculture Products Using Liquid Chromatography-Tandem Mass Spectrometry, *Frontiers in nutrition*, 2021, **8**, 812803.

16. S. Wu, H. Zhang, Z. Shi, N. Duan, C. Fang, S. Dai and Z. Wang, Aptamer-based fluorescence biosensor for chloramphenicol determination using upconversion nanoparticles, *Food Control*, 2015, **50**, 597-604.

17. A. Yamagishi, F. Ito and C. Nakamura, Study on Cancer Cell Invasiveness via Application of Mechanical Force to Induce Chloride Ion Efflux, *Analytical Chemistry*, 2021, **93**, 9032-9035.

18. A. Ruscito and M. C. DeRosa, Small-Molecule Binding Aptamers: Selection Strategies, Characterization, and Applications, *Frontiers in chemistry*, 2016, **4**, 14.

19. A. K. Sharma and J. M. Heemstra, Small-Molecule-Dependent Split Aptamer Ligation, *Journal of the American Chemical Society*, 2011, **133**, 12426-12429.

20. H. Yu, O. Alkhamis, J. Canoura, Y. Liu and Y. Xiao, Advances and Challenges in Small-Molecule DNA Aptamer Isolation, Characterization, and Sensor Development, *Angewandte Chemie (International ed. in English)*, 2021, **60**, 16800-16823.

21. X. Yang, C. H. Chan, S. Yao, H. Y. Chu, M. Lyu, Z. Chen, H. Xiao, Y. Ma, S. Yu, F. Li, J. Liu, L. Wang, Z. Zhang, B.-T. Zhang, L. Zhang, A. Lu, Y. Wang, G. Zhang and Y. Yu, DeepAptamer: Advancing high-affinity aptamer discovery with a hybrid deep learning model, *Molecular Therapy Nucleic Acids*, 2025, **36**, 102436.

22. Y. Ding and J. Liu, Pushing Adenosine and ATP SELEX for DNA Aptamers with Nanomolar Affinity, *Journal of the American Chemical Society*, 2023, **145**, 7540-7547.

23. Y. Zhang, L. Zhu, X. Ma, S. Zhu, Y. Ma, S. Hussain, X. He and W. Xu, An Effective Docking-Guided Strategy for Rational Tailoring of Fluorescent Aptamer Switches of Dimethylindole Red Analogue, *Analytical Chemistry*, 2023, **95**, 7076-7081.

24. L. F. M. Passalacqua, M. R. Starich, K. A. Link, J. Wu, J. R. Knutson, N. Tjandra, S. R. Jaffrey and A. R. Ferré-D'Amaré, Co-crystal structures of the fluorogenic aptamer Beetroot show that close homology may not predict similar RNA architecture, *Nature Communications*, 2023, **14**.

25. H. Chen, Y. Li, Z. Xiao, J. Li, T. Li, Z. Wang, Y. Liu and W. Tan, Chemical Amplification-Enabled Topological Modification of Nucleic Acid Aptamers for Enhanced Cancer-Targeted Theranostics, *ACS Nano*, 2023, **17**, 17740-17750.

26. R. Nutiu and Y. Li, In Vitro Selection of Structure‐Switching Signaling Aptamers, *Angewandte Chemie International Edition*, 2005, **44**, 1061-1065.

27. H.-R. Chen, M.-L. Su, Y.-M. Lei, Z.-X. Ye, Z.-P. Chen, P.-Y. Ma, R. Yuan, Y. Zhuo, C.-Y. Yang and W.-B. Liang, Insights of Life Molecules' Dynamic Distribution in Live Cells via Sequence–Structure Bispecific Fluorescent RNA, *Journal of the American Chemical Society*, 2023, **145**, 12812-12822.

28. Z. Luo, Y. Li, P. Zhang, L. He, Y. Feng, Y. Feng, C. Qian, Y. Tian and Y. Duan, Catalytic hairpin assembly as cascade nucleic acid circuits for fluorescent biosensor: Design, evolution and application, *TrAC Trends in Analytical Chemistry*, 2022, **151**.

29. F. C. Simmel, B. Yurke and H. R. Singh, Principles and Applications of Nucleic Acid Strand Displacement Reactions, *Chemical Reviews*, 2019, **119**, 6326-6369.

30. Y. Si, L. Xu, T. Deng, J. Zheng and J. Li, Catalytic Hairpin Self-Assembly-Based SERS Sensor Array for the Simultaneous Measurement of Multiple Cancer-Associated miRNAs, *ACS Sensors*, 2020, **5**, 4009-4016.

31. F. Ma, C.-C. Li and C.-Y. Zhang, Nucleic acid amplification-integrated single-molecule fluorescence imaging forin vitroandin vivobiosensing, *Chemical Communications*, 2021, **57**, 13415-13428.

32. C. A. Cox, A. N. Ogorek, J. P. Habumugisha and J. D. Martell, Switchable DNA Photocatalysts for Radical Polymerization Controlled by Chemical Stimuli, *Journal of the American Chemical Society*, 2023, **145**, 1818-1825.

33. A. J. Genot, D. Y. Zhang, J. Bath and A. J. Turberfield, Remote Toehold: A Mechanism for Flexible Control of DNA Hybridization Kinetics, *Journal of the American Chemical Society*, 2011, **133**, 2177-2182.

34. A. D. Ellington and J. W. Szostak, In vitro selection of RNA molecules that bind specific ligands, *Nature*, 1990, **346**, 818-822.

35. Y. S. Jiang, S. Bhadra, B. Li and A. D. Ellington, Mismatches improve the performance of strand-displacement nucleic Acid circuits, *Angewandte Chemie (International ed. in English)*, 2014, **53**, 1845-1848.

View Article Online
DOI: 10.1039/D5SC04624F

36. Q. Liu, Y. Huang, Z. Li, L. Li, Y. Zhao and M. Li, An Enzymatically Gated Catalytic Hairpin Assembly Delivered by Lipid Nanoparticles for the Tumor-Specific Activation of Signal Amplification in miRNA Imaging, *Angewandte Chemie International Edition*, 2022, **61**, e202214230.
37. Y. Zhang, C. Yang, J. He, S. Zuo, X. Shang, J. Gao, R. Yuan and W. Xu, Target DNA-Activating Proximity-Localized Catalytic Hairpin Assembly Enables Forming Split-DNA Ag Nanoclusters for Robust and Sensitive Fluorescence Biosensing, *Analytical Chemistry*, 2022, **94**, 14947-14955.
38. Z. Weng, H. Yu, W. Luo, Y. Guo, Q. Liu, L. Zhang, Z. Zhang, T. Wang, L. Dai, X. Zhou, X. Han, L. Wang, J. Li, Y. Yang and G. Xie, Cooperative Branch Migration: A Mechanism for Flexible Control of DNA Strand Displacement, *ACS Nano*, 2022, **16**, 3135-3144.
39. L. Deng, Y. Wu, S. Xu, Y. Tang, X. Zhang and P. Wu, Improving the Signal-to-Background Ratio during Catalytic Hairpin Assembly through Both-End-Blocked DNAzyme, *ACS Sensors*, 2018, **3**, 1190-1195.
40. L. Zhao, Y. Song and H. Xu, Catalytic hairpin self-assembly for biosensing: Classification, influencing factors, and applications, *TrAC Trends in Analytical Chemistry*, 2024, **171**, 117508.
41. J. Mehta, B. Van Dorst, E. Rouah-Martin, W. Herrebout, M.-L. Scippo, R. Blust and J. Robbens, In vitro selection and characterization of DNA aptamers recognizing chloramphenicol, *Journal of Biotechnology*, 2011, **155**, 361-369.
42. Y. Zhang, W.-G. Yang, M.-L. Su, B.-W. Wang, R. Yuan and W.-B. Liang, A reagent-based label free electrochemiluminescence biosensor for ultrasensitive quantification of low-abundant chloramphenicol, *Microchemical Journal*, 2024, **198**.
43. T. Mayer, L. Oesinghaus and F. C. Simmel, Toehold-Mediated Strand Displacement in Random Sequence Pools, *Journal of the American Chemical Society*, 2023, **145**, 634-644.
44. N. Srinivas, T. E. Ouldridge, P. Šulc, J. M. Schaeffer, B. Yurke, A. A. Louis, J. P. K. Doye and E. Winfree, On the biophysics and kinetics of toehold-mediated DNA strand displacement, *Nucleic Acids Research*, 2013, **41**, 10641-10658.

View Article Online
DOI: 10.1039/D5SC04624F

All the data supporting the findings of this study are available within the article and can be obtained from the corresponding author upon reasonable request.